Beamforming demonstration of Hybrid Photonic Integrated Circuit based on a Blass Matrix for Radar receivers

Federico Camponeschi[1], Valentina Gemmato[1], Filippo Scotti[2], Luca Rinaldi[2], Ahmad W. Mohammad[3], Chris G. Roeloffzen[3], Paul W. van Dijk[3] and Paolo Ghelfi[2]
[1]Scuola Superiore Sant'Anna, Via Moruzzi 1, 56124 Pisa, Italy
[2]CNIT, Via Moruzzi 1, 56124 Pisa, Italy
[3]LioniX International, Enschede, The Netherlands
federico.camponeschi@santannapisa.it

Abstract: This paper reports the first-ever beamforming demonstration of a hybrid photonic integrated circuit operating as RF down-converter based on an optical Blass-matrix architecture for a Scan-on-Receive synthetic aperture radar intended for Earth observation from space.

1. Introduction

In recent decades, Earth observation (EO) technology has played a vital role in gathering extensive global data for climate change research and for monitoring natural resources [1]. One widely used EO technique is synthetic aperture radar (SAR), which provides radar-based elevation images independently of weather conditions and time of day and operates in various microwave frequency bands depending on the application [2]. Advanced SAR imaging modes now incorporate beam steering capabilities in spaceborne SAR sensors, achieved through RF analog, digital, or hybrid methods. Digital beam steering, however, faces challenges related to cost, size, and power consumption, limiting its use to larger spacecraft [3]. Recent advancements in microwave photonics and photonic integrated circuit (PIC) technology offer a promising compact, broadband, and low-loss alternative for implementing radar beam steering, making SAR viable for smaller missions [4, 5]. Future spaceborne SAR instruments aim to perform instantaneous wide swath imaging at high resolution, a goal attainable through advanced SAR imaging modes like scan-on-receive (SCORE). SCORE involves illuminating a wide swath during the transmit mode and steering multiple receive beams simultaneously across the swath to capture radar echoes from different transmit events [6].

This paper presents the demonstration of beamforming capability of a photonics-based SCORE-SAR receiver module developed within the SPACEBEAM project [7]. The project's objective is to achieve a swath width five times larger than existing spaceborne SAR systems while maintaining a spatial resolution of 1.5 meters in both along- and across-track directions [8]. SPACEBEAM offers reconfigurable 12x3 beamforming and signal down-conversion capabilities, utilizing a Blass matrix [9]. The target frequency is 9.65 GHz in the X-band with a minimum bandwidth of 450 MHz. The receiver module is similar to the one described in [10], with the sole difference being the use of heater-based phase shifters in place of Lead Zirconate Titanate (PZT) actuators. While employing heater-based actuators results in significantly higher power consumption and slower tuning speed, their technological maturity enables the comprehensive characterization of this receiver, including beamforming capabilities. To the best of our knowledge, these are the first-ever experimental results of a fully integrated optical beamforming network based on a Blass-matrix architecture.

2. Architecture description

The implemented architecture serves as 12x3 beamformer for a SCORE-SAR receiver operating in the X-band at

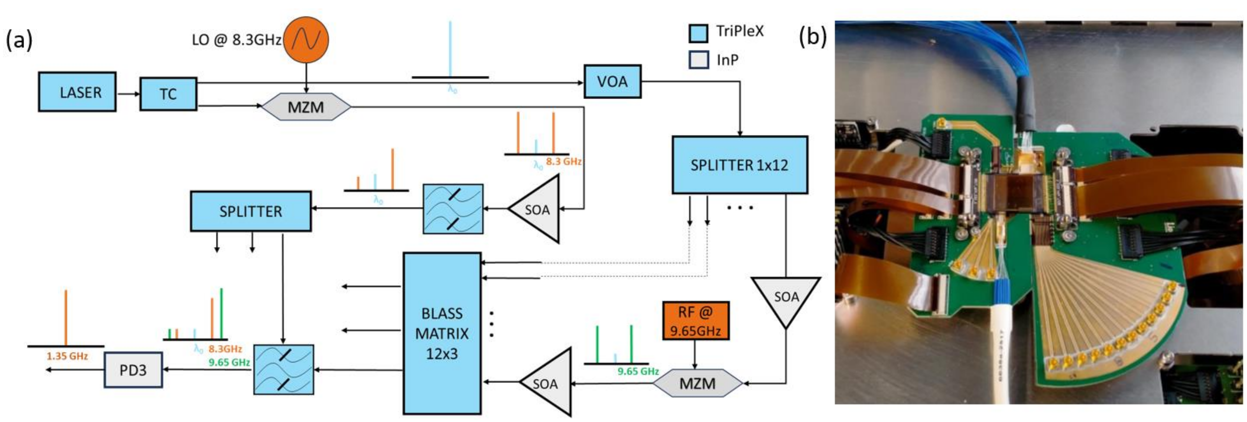

Fig. 1: (a) schematic diagram of the implemented architecture and (b) a photo of the hybrid assembly.

9,65 GHz, featuring the capability to down-convert to a 1,35 GHz intermediate frequency (IF) signal. In the schematic depicted in Fig. 1 (a), the laser power is divided by a tunable coupler. One branch directs power to the LO modulator, while the other directs it towards the RF modulators. Both modulator chips are provided with semiconductor optical amplifiers (SOAs). The modulators employed are push-pull Mach–Zehnder modulators (MZM) with dual outputs and are biased at the null point. On the RF path, the double sideband suppressed carrier signal is filtered by a fifth order ring-assisted Mach-Zehnder interferometer (RAMZI) in order to eliminate one of the two sidebands. Meanwhile, on the other path, the laser signal is split into 12 channels composed by a SOA-MZM-SOA chain so that 12 RF input signals coming from 12 input antennas are received. Subsequent to modulation and amplification, the RF-modulated optical signals converge within the 12x3 Blass matrix which performs delay, phase and amplitude control to the modulated signals, combining them to create the 3 received beams. The 3 Blass matrix outputs pass through 3 RAMZI filters, which select the sidebands of the RF modulation and the filtered sideband coming from the LO path. Finally, these two signals are heterodyned in the photodiodes (PDs), resulting in the generation of the down-converted IF signal.

The proposed design incorporates active components on indium phosphide (InP) and passive components on silicon nitride (Si_3N_4). In particular, the fabricated PIC is a hybrid integration of a Si_3N_4 chip (TriPleX®) which provides low-loss waveguides, signal filtering, signal splitting, combining, and optical beamforming network along with 4 InP chips. These InP chips include the gain section of the laser, the array of MZMs integrated with SOAs and an array of PDs. A picture of the hybrid assembly with the printed circuit board (PCB) is displayed in Fig. 1 (b).

3. Experimental characterization

Firstly, the down-conversion functionality was assessed. The laser, SOAs, LO modulation, and one of the 12 RF modulation channels were activated. An 8.3 GHz, 18 dBm LO signal was provided by a signal generator, while the RF signal was generated by a second source set at 9.65 GHz with a power of 10 dBm. The filters were appropriately adjusted, and the Blass matrix was configured to direct the signal to the nearest output. The down-converted signal was measured using an ESA at 1.35 GHz, and its power was recorded as -40 dBm, resulting in a conversion gain of -45 dB, which includes losses attributed to the PCB and RF cables. The consistent enhancement in conversion gain compared to the results obtained in the PZT-based version of the receiver module [10] can be attributed to the higher laser power in our case, which is approximately 18 dBm, as opposed to the -11.8 dBm in the previous version. Furthermore, the deviation from the target simulated conversion gain value of -27.7 dB [10] can largely be attributed to the losses at the Si_3N_4-InP interface. The measured loss value was 6.5 dB, whereas the simulated value was 4 dB.

Then, the beamforming functionality of the PIC receiver module was evaluated. A 1x3 subset of the Blass matrix was employed as to interface with a 3 elements array antenna. Inside the PIC, inputs from the 3 RF channels are properly phase and amplitude adjusted so that they sum to output a single signal. To emulate incoming RF waves, the RF signal form a single synthesizer was divided into three arms and their phases were adjusted using RF delay lines to simulate the angle of the incoming RF signal, according to the beamforming equation:

$$\tau_n = \tau_{n-1} + \pi \,\mathrm{sen}\theta \tag{1}$$

that is valid when the spacing between elements is exactly one half of the signal wavelength, as sketched in Fig. 2 (a). The phase shifters within the Blass matrix were then tuned to align the PIC so that the emulated array antenna points in the θ direction. To minimize the adverse effects of thermal crosstalk arising from the adjustment of the Blass matrix actuators, which can cause detuning of the laser frequency and filters, an external laser was utilized. Moreover, the filters, also suffering the thermal crosstalk, were tuned to achieve a flat response. The signal collected

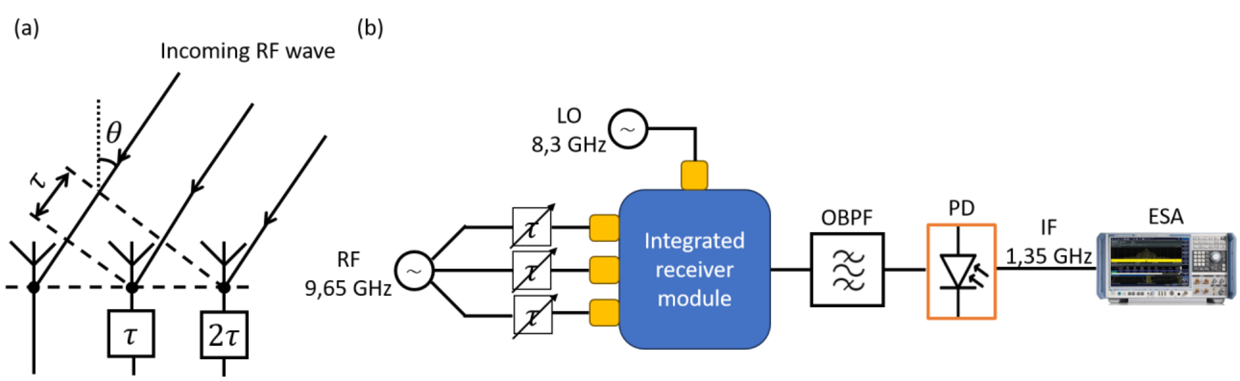

Fig. 2: (a) Operation principle of the generic beamformer (b) and scheme of the measurement setup.

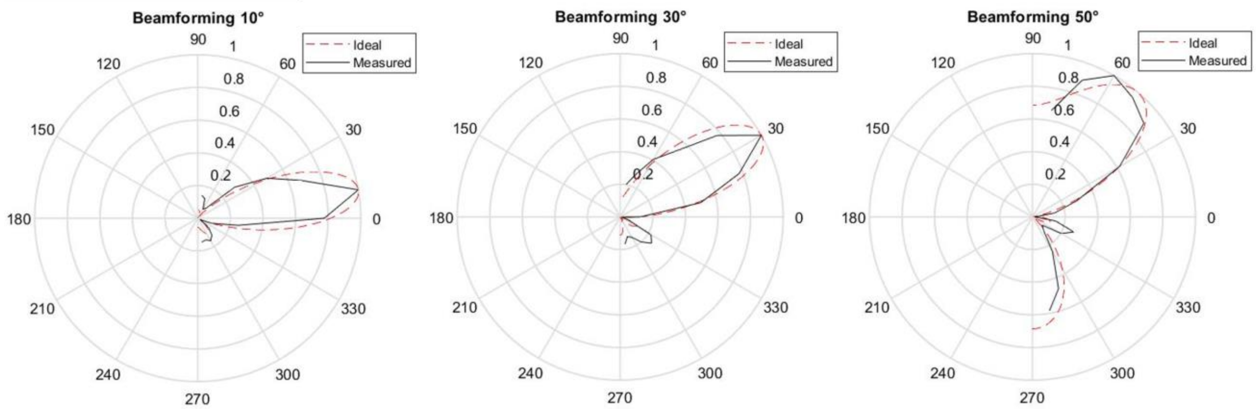

Fig. 3: polar diagrams of the received beams with the Blass matrix set to 10°, 30° and 50° pointing directions

from a monitoring optical output was then filtered externally to eliminate the undesired sidebands, detected by a photodiode (PD), and measured using an ESA. The measurement setup is illustrated in Fig. 2 (b).

Subsequently, different pointing directions for incoming the RF waves were emulated, and the down-converted output power was recorded to create a radiation diagram representing the received signal. In the first measurement, the Blass matrix phase shifters were adjusted to the required phase shifts for pointing in the 10° direction. According to Equation (1), phase shifts of 31.26° and 62.52° were applied between the first and second antenna elements and between the second and third antenna elements, respectively. Then, the pointing angles θ of the input RF signal were systematically scanned from -80° to 80° to measure an antenna diagram. The same measurement procedure was repeated with the Blass matrix set to 30° and 50° pointing directions. In Fig. 3, radiation diagrams obtained with the beamforming network set at 10°, 30°, and 50° are presented in comparison with the ideal plots. Deviations from the ideal plot are primarily due to the imperfect power matching of the three RF signals combined within the Blass matrix.

4. Conclusions

This paper presented the first-ever beamforming demonstration of a hybrid photonic integrated circuit designed as a receiver based on an optical Blass-matrix architecture for a Scan-on-Receive synthetic aperture radar intended for Earth observation from space. The Spacebeam assembly has been described and the experimental setup and results are reported, including down-conversion of the input X-band RF signal and polar diagrams of the received beams changing the Blass matrix pointing direction. Comparison with the ideal pattern of a perfect beamformer are also reported, confirming the effectiveness of the proposed scheme. Further experimental tests will address the capability of the implemented optical beamforming network to receive multiple beams.

5. References

[1] H.-D. Guo, L. Zhang, and L.-W. Zhu, “Earth observation big data for Climate Change Research”, in *Advances in Climate Change Res.*, vol. 6, no. 2, pp. 108–117, 2015. doi:10.1016/j.accre.2015.09.007.

[2] A. Moreira, P. Prats-Iraola, M. Younis, G. Krieger, I. Hajnsek and K. P. Papathanassiou, "A tutorial on synthetic aperture radar," in *IEEE Geosci. Remote Sens. Mag.*, vol. 1, no. 1, pp. 6-43, March 2013, doi: 10.1109/MGRS.2013.2248301.

[3] S. Kutty and D. Sen, “Beamforming for Millimeter Wave Communications: An inclusive survey”, *IEEE Communications Surveys & Tutorials*, vol. 18, no. 2, pp. 949–973, 2016. doi:10.1109/comst.2015.2504600.

[4] P. Ghelfi et al., “A fully photonics-based coherent radar system”, *Nature*, vol. 507, no. 7492, pp. 341–345, 2014. doi:10.1038/nature13078.

[5] S. Li et al., “Chip-based microwave-photonic radar for high-Resolution Imaging,” *Laser & Photonics Reviews*, vol. 14, no. 10, p. 1900239, 2020. doi:10.1002/lpor.201900239.

[6] T. Otto et al., "Microwave Photonics Beamformer for Spaceborne SAR," *EUSAR 2022*; 14th European Conference on Synthetic Aperture Radar, Leipzig, Germany, 2022, pp. 1-3.

[7] “Space SAR system with reconfigurable integrated photonic beamforming”, SPACEBEAM, https://www.spacebeam-project.eu/ (accessed Jun. 5, 2023).

[8] M. Reza et al., “Design and performance estimation of a photonic integrated beamforming receiver for scan-on-receive Synthetic Aperture Radar,” *J. Lightw. Technol.*, vol. 39, no. 24, pp. 7588–7599, 2021. doi:10.1109/jlt.2021.3119225.

[9] C. Tsokos et al., “Analysis of a multibeam optical beamforming network based on Blass Matrix Architecture,” *J. Lightw. Technol*., vol. 36, no. 16, pp. 3354–3372, 2018. doi:10.1109/jlt.2018.2841861.

[10] A. W. Mohammad et al., "Design, Fabrication, and Characterization of a Hybrid Integrated Photonic Module for a Synthetic Aperture Radar Receiver," in *Journal of Lightwave Technology*, doi: 10.1109/JLT.2023.3318473.